Progress In Electromagnetics Research Letters, Vol. 68, 53–58, 2017

A Logarithmic Version of the Complex Generalized Smith Chart

Pablo Vidal-García* **and Emilio Gago-Ribas**

Abstract—Based on the complex analysis of the Lossy Transmission Line Theory, which involves the result of a Generalized Smith Chart, whose new version arises when trying to characterize the wave impedance along the Transmission Line by means of analytical complex functions. Among these functions, the complex logarithm of the reflection coefficient leads to the logarithmic-reflexion coefficient-plane and its parameterized version, the Logarithmic Generalized Smith Chart. This plane is specially useful for characterizing the Transmission Line along its extension. To validate these results, some examples will be presented providing physical interpretations to the behaviour of a lossy TL and pointing out some practical applications.

1. INTRODUCTION

The *Complex Transmission Line Theory* (CTLT) [1], based on the complex variable analysis, has demonstrated its usefulness characterizing the Transmission Line (TL) parameters as well as providing physical behaviors of the TL when losses are taken into account [1, 2], leading to a rigorous characterization which overcomes the limitations inherent to the usual *Transmission Line Theory* (TLT) and also providing new uses of losses in RF circuit design. However, it is common that the more accurate and deeper the lossy characterization and used models are, the more difficult is to analyze the parameters on the TL. In order to avoid these complexities, the CTLT makes use of the: (i) normalizations of the TL parameters that allow to group TLs with common properties — e.g., TLs with the same conductor/dielectric losses — represented by 'universal' curves; (ii) graphical characterizations which reduce the analysis to geometrical operations in the complex planes associated to each parameter; and (iii) transformations between these planes seen as conformal complex mappings.

One of the most used maps in the TLT is the transformation between the reflection coefficient ρ-plane and the wave impedance Z_n-plane, $Z_n = Z/Z_0$, $Z_0 \in \Re$, which leads to the usual Smith Chart (SC) for the lossless case [3, 4], and some extended versions which show practical usefulness when analyzing different circuits [6, 7]. The CTLT generalizes this transformation when losses are included by means of the Generalized Smith Chart (GSC) [5]. This case assumes the normalization $Z_n = Z/|Z_0|$ which recalls the importance of φ_{Z_0} in the analysis of lossy TLs because of the parameter which determines the particular GSC depending on losses [1, 5]. Since the GSC is useful for characterizing the TL *point by point* — e.g., the transformations between ρ and Z_n in single points along the TL — some lacks appear in the analysis along the lossy TL in which the parameter γ — and in particular φ_γ — describes the behavior of ρ along its extension.

To avoid such limitations and to afford the study of the wave parameters along the TL by means of fully geometrical operations, a logarithmic version of the GSC (log-GSC), in which φ_γ directly appears, is proposed in this paper. In Section 2, the characterization of $Z_n(l)$ in terms of complex functions will be justified by explaining the bases of the log-GSC depicted in the $\rho_{\log}$-plane. In Section 3, the relevant transformations between planes ρ and Z_n and $\rho_{\log}$-plane will be reviewed emphasizing the direct

Received 20 February 2017, Accepted 27 April 2017, Scheduled 24 May 2017
* Corresponding author: Pablo Vidal-García (pvidal@tsc.uniovi.es).
The authors are with the Department of Electrical, Electronic, Computers and Systems Engineering, Signal Theory and Communications Area, University of Oviedo, 33203-Gijón, Asturias, Spain.

geometrical transformations concerning ρ and $\rho_{\log}$ in the study along the TL. Finally, some examples involving the $\rho_{\log}$-plane will be presented in Section 4 providing physical interpretations associated to losses in the TLT.

2. THE BASES OF THE log-GSC

2.1. Z_n as Complex Function of $\rho_{\log}$

Let us begin with the the well-known general equation of Z along the TL,

$$Z(l) = Z_0 \frac{Z_L \cosh(\gamma l) + Z_0 \sinh(\gamma l)}{Z_0 \cosh(\gamma l) + Z_L \sinh(\gamma l)}, \tag{1}$$

with Z_0, $Z_L = Z(l=0)$ and γ complex, and $l = 0$ represents the position at the load (the end of the TL), as usual. Eq. (1) is intrinsically difficult to characterize, so the usual alternative study is done by means of

$$\rho(l) = \rho_L e^{-2\gamma l} \quad \text{with} \quad \rho_L = \rho(l=0) = m_L e^{j\varphi_{\rho_L}} = \frac{Z_L - Z_0}{Z_L - Z_0}, \tag{2}$$

which describes $Z(l)$ in terms of $\rho(l)$ through the linear fractional transformation

$$Z(l) = Z_0 \frac{1+\rho(l)}{1-\rho(l)}. \tag{3}$$

Last equation is quite simpler to analyze than that in Eq. (1). In addition, the normalization Z_n as defined above, which generalizes the behavior of Z [1], allows the study of 'universal' curves of Z_n keeping the definition of ρ and reducing the parameterization to φ_{Z_0},

$$Z_n(l) = e^{j\varphi_{Z_0}} \frac{1+\rho(l)}{1-\rho(l)}. \tag{4}$$

The particular analysis performed in [1] parameterizing Z_n in its real ($Z_n' = a$) and imaginary ($Z_n'' = b$) parts leads to the GSC [1, 5]. Taking the modulus, m, and phase, p, of the reflection coefficient in Eq. (2) and connecting both by solving l leads to the well-known logarithmic spiral,

$$|\rho| = m = m_L e^{\frac{\alpha}{\beta}(\varphi_{\rho_L} - p)} \quad \text{with} \quad p \leq \varphi_{\rho_L}, \tag{5}$$

in which let $Z_n(l)$ be represented by parametric equations given by geometrical intersections between m- and p-circumferences [1]. Now, the alternative analysis based on complex analytical functions is done by substituting Eq. (2) in Eq. (4) and using the complex analytical functions $\log(\circ)$ and $\coth(\circ)$, leading to:

$$\begin{aligned} Z_n(l) &= e^{j\varphi_{Z_0}} \frac{1 + e^{\log(\rho_L) - 2\gamma l}}{1 - e^{\log(\rho_L) - 2\gamma l}} = e^{j\varphi_{Z_0}} \frac{e^{-[\frac{1}{2}\log(\rho_L) - \gamma l]} + e^{\frac{1}{2}\log(\rho_L) - \gamma l}}{e^{-[\frac{1}{2}\log(\rho_L) - \gamma l]} - e^{\frac{1}{2}\log(\rho_L) - \gamma l}} \\ &= -e^{j\varphi_{Z_0}} \coth\left[\frac{1}{2}\log(\rho_L) - \gamma l\right] = -e^{j\varphi_{Z_0}} \coth \underbrace{\left[\frac{1}{2}\log(m_L) - \alpha l + j\left(\frac{1}{2}\varphi_{\rho_L} - \beta l\right)\right]}_{\rho_{\log}} \end{aligned} \tag{6}$$

Notice that the argument of $\coth(\circ)$ separates the effects of losses and propagation with the real and imaginary parts affecting m_L and φ_{ρ_L}, respectively. The argument of the function $\coth(\circ)$ is named $\rho_{\log}$ defined as,

$$\rho_{\log} \equiv \frac{1}{2}\log(\rho) = \frac{1}{2}\left[\log(|\rho|) + j\varphi_\rho\right], \quad \text{to} \quad \begin{cases} \operatorname{Re}\{\rho_{\log}\} < m_L \\ \operatorname{Im}\{\rho_{\log}\} < \varphi_{\rho_L} \end{cases}, \tag{7}$$

forming a conformal map in the branch cut of $\log(\circ)$ chosen by fixing $\varphi_{\rho_{\log}} \in [0, \pi[$ (see Fig. 4). Since $\coth(\circ)$ is an entire complex function, $\rho_{\log}$ may be seen as the variable in which losses and propagation along the TL are described in terms of the initial and final points. Notice also from Eq. (6) that $\rho_{\log}$ is a line in the $\rho_{\log}$-plane parameterized by l (see Fig. 4). Thus, the analysis along the TL performed in this plane, i.e., the log-GSC, is more affordable than in the GSC.

Table 1. Summary of the main transformations between complex ρ-, $\rho_{\log}$- and Z_n-planes.

ρ-plane	$\rho_{\log}$-plane		
$\lvert\rho\rvert = m$	$\rho'_{\log} = \frac{1}{2}\log(m),\ m \in \left]0, \frac{c_0}{1-s_0}\right]$	$\rho''_{\log} \in \begin{cases} \frac{\pi}{2} - \frac{1}{2}\sin^{-1}\left(\frac{1-m^2}{2mt_0}\right) \text{ if } t_0 \neq 0,\ m \geq \frac{c_0}{1+s_0} \\ [0, \pi[, \text{ otherwise} \end{cases}$	(a)
$\varphi_\rho = p$	$\rho'_{\log} \in \left]-\infty, \frac{1}{2}\log\left(-t_0\sin(p) + \sqrt{1+t_0^2\sin^2(p)}\right)\right]$	$\rho''_{\log} = \frac{p}{2},\ p \in [0, \pi[$	

$\rho_{\log}$-plane	Z_n-plane		
	General Equation	Parametric Circumferences, (center): radius	
$\rho'_{\log} = a$	$\left(Z'_n + c_0\frac{(e^{2a})^2+1}{(e^{2a})^2-1}\right)^2 + \left(Z''_n + s_0\frac{(e^{2a})^2+1}{(e^{2a})^2-1}\right)^2 = \left(\frac{2e^{2a}}{(e^{2a})^2-1}\right)^2$	$\left(-c_0\frac{(e^{2a})^2+1}{(e^{2a})^2-1}, -s_0\frac{(e^{2a})^2+1}{(e^{2a})^2-1}\right) : \frac{2e^{2a}}{\lvert(e^{2a})^2-1\rvert}$	(b)
$\rho''_{\log} = b$	$\left(Z'_n + \frac{c_0}{\tan(2b)}\right)^2 + \left(Z''_n - \frac{s_0}{\tan(2b)}\right)^2 = \left(\frac{1}{\sin(2b)}\right)^2$	$\left(-\frac{c_0}{\tan(2b)}, \frac{s_0}{\tan(2b)}\right) : \frac{1}{\lvert\sin(2b)\rvert}$	

Z_n-plane	$\rho_{\log}$-plane		
$Z'_n = a$	$\rho'_{\log} = -\frac{1}{2}\log\left(\frac{a\cos(2\rho''_{\log}) - s_0\sin(2\rho''_{\log}) + \sqrt{1-\left(s_0\cos(2\rho''_{\log}) + a\sin(2\rho''_{\log})\right)^2}}{a+c_0}\right)$	$\rho''_{\log} \in [0, \pi[$	(c)
$Z''_n = b$	$\rho'_{\log} = -\frac{1}{2}\log\left(\frac{b\cos(2\rho''_{\log}) - c_0\sin(2\rho''_{\log}) + \sqrt{1-\left(c_0\cos(2\rho''_{\log}) + b\sin(2\rho''_{\log})\right)^2}}{b-c_0}\right)$	$\rho''_{\log} \in [0, \pi[$	

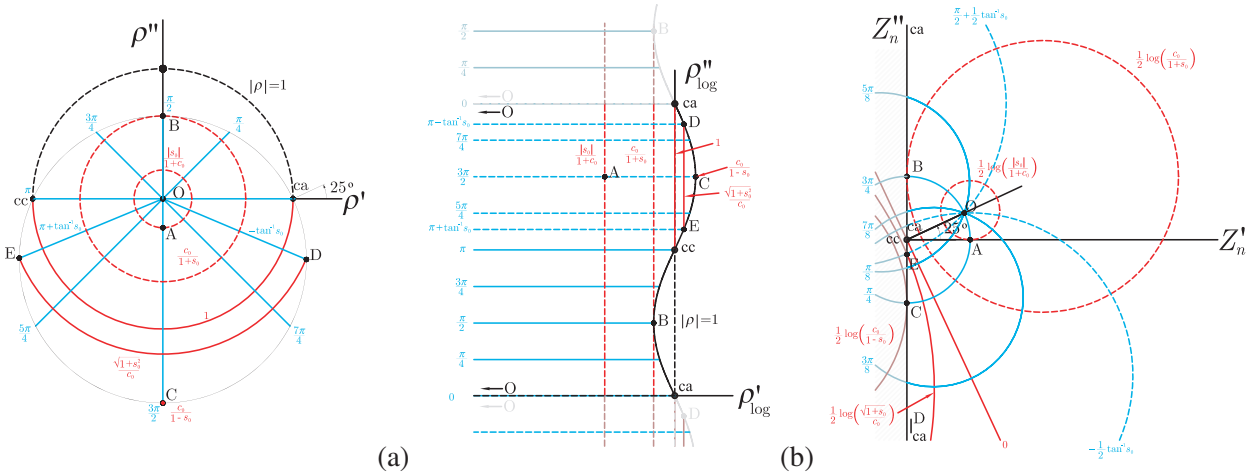

Figure 1. Graphical analysis of the modulus and phase from (a) the ρ-plane to the $\rho_{\log}$-plane — an example of the curves in Table 1(a) when $\varphi Z_0 = 25°$ and (b) from the $\rho_{\log}$-plane to the Z_n-plane.

3. COMPLEX TRANSFORMATIONS BETWEEN PLANES

Once the log-GSC has been introduced together with the relations between ρ and Z_n by means of Eqs. (7) and (6), respectively, the graphical analysis is done by parameterizing the real and imaginary parts, as well as the modulus and phase of each parameter and geometrically studying the resulting curves (the same metodology used in [1] and [5]). The most important transformations may be summarized as follows.

3.1. Analysis of Z_n from $\rho_{\log}$

This analysis leads to representing Z_n along the TL, studying the reflection coefficient from $\rho_{\log}$ instead of ρ and avoiding the use of Eq. (5). Solving $\rho_{\log}$ from Eq. (6),

$$\rho_{\log} = \frac{1}{2}\log\left(\frac{1 + Z_n e^{j\varphi z_0}}{1 - Z_n e^{j\varphi z_0}}\right), \tag{8}$$

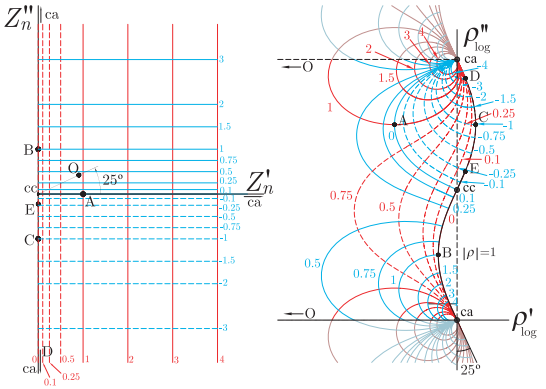

Figure 2. Graphical analysis of the real and imaginary parts from the Z_n-plane to the $\rho_{\log}$-plane conforming the log-GSC.

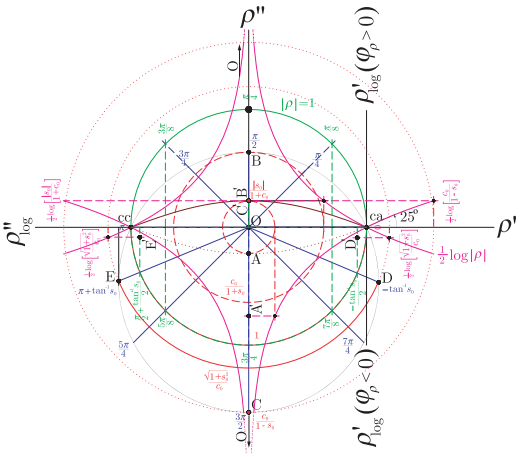

Figure 3. Example of a procedure to relate both the ρ- and the $\rho_{\log}$-planes.

and parameterizing the real and imaginary parts of $\rho_{\log}$, leads to the results in Table 1(b) and Fig. 1(b). The $\rho''_{\log}$-curves in Fig. 1(b) are $\frac{\pi}{2}$-periodically overlapped, whereas $\rho'_{\log}$-curves tend to point O when their values decrease. Both are sloped by φ_{Z_0} and geometrically connected by φ_γ in the $\rho_{\log}$-plane when studying them along the TL.

3.2. Analysis of $\rho_{\log}$ from ρ

This analysis is carried out parameterizing the modulus and phase of ρ as indicated in Table 1(a). Main curves locating points O and A-E in the ρ-plane have been transformed into the $\rho_{\log}$-plane as shown in Fig. 1(a). Notice that the $\rho_{\log}$-plane is left-opened when approaching to point O leading to the idea of being possible to add equal length-scales along the TL.

3.3. Analysis of $\rho_{\log}$ from Z_n: The log-GSC

Parameterizing the real and imaginary parts of Z_n in Eq. (6) leads to the expressions summarized in Table 1(c) and depicted in Fig. 2. The complexity of the parameterized expressions in Table 1(c) leads to the use of the GSC instead of the log-GSC when composing impedances graphically.

4. EXAMPLES OF USE

Some examples using the log-GSC are presented then in order to remark the usefulness which provide for the analysis of the wave parameters along the TL, operating together with the ρ- and Z_n-planes.

4.1. Graphical Procedure to Relate ρ- and the $\rho_{\log}$-planes

The convenience of using the $\rho_{\log}$-plane instead of the ρ-plane has been seen in the analysis of the wave parameters along the TL.

However, the use of $\rho_{\log}$-plane lacks some facilities provided by the GSC, e.g., the simplicity of curves — circumferences [1] —- parameterizing impedances from the Z_n-plane. Thus, a direct graphical procedure to relate ρ- and $\rho_{\log}$-planes becomes very useful. In this sense, each plane will support the other emphasizing its own usefulness. In Fig. 3, an intuitive procedure to transform ρ- and $\rho_{\log}$-planes is presented in the same graph. Modulus transformations are depicted in red and magenta, whereas phase transformations are coloured in blue and green, and supported by the eye-pattern curves $\frac{1}{2}\log(\rho)$ and $\rho = 1$ added in solid magenta and green, respectively. Remarkable point transformations are between A-E and O and their primes, and may be seen turning the page clockwise by following the dashed lines.

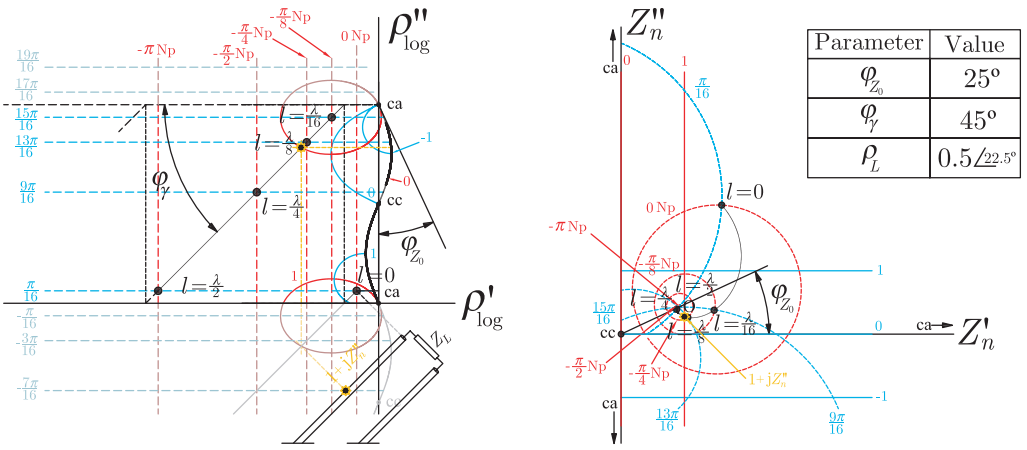

Figure 4. An example of the graphical analysis along the TL using of the $\rho_{\log}$- and Z_n-planes.

The example in Fig. 3 shows the $\rho_{\log}$-plane usefulness through the characterization of ρ along the TL leading to adding wavelength scales easily and highlighting some a priori hidden physical interpretations. Notice that the $\rho_{\log}$-plane has been folded, which is possible since $\varphi_\rho \geq 0$ and $\varphi_\rho \leq 0$ regions do not overlap each other in the $\rho_{\log}$-plane with the exception of their common boundary. Thus, the maximum and minimum in the folded $\rho_{\log}$-plane (denoted by B' and C') are located in the same point. This compact representation may be useful when trying to relate the log-GSC and the GSC.

4.2. Analysis along the TL

In Fig. 4, the spiral of Eq. (6) in the Z_n-plane has been obtained going over the straight line which represents the TL in the $\rho_{\log}$-plane, as well as adding regular scales in terms of λ. Notice that, since TL losses are fixed, the curve in the $\rho_{\log}$-plane keeps up the angles φ_{Z_0} and φ_γ. To the truly physical realizability of the TL, these angles have to fulfil the following conditions,

$$\begin{aligned} 0 \leq \varphi_\gamma + \varphi_{Z_0} \leq \frac{\pi}{2} \quad \text{and} \\ 0 \leq \varphi_\gamma - \varphi_{Z_0} \leq \frac{\pi}{2}, \end{aligned} \tag{9}$$

because of the normalized lossy model proposed [1]. Through the double condition in Eq. (9), the values of r and g are fixed, so the inverse characterization of the TL in terms of the line parameters may be rapidly deduced from the $\rho_{\log}$-plane (see the next example concerning matching impedances with lossy TLs).

4.3. Impedance Matching with Lossy TLs

By means of this example, the most practical use of the $\rho_{\log}$-plane and lossy TLs matching the impedance Z_M from any impedance at the load Z_L is pointed out.

The analysis in Fig. 5 follows the procedure: (i) by fixing an arbitrary φ_{Z_0} (e.g., $\varphi_{Z_0} = 25°$), $\rho_{\log L}$ and the desired $\rho_{\log M}$ are located in the $\rho_{\log}$-plane. From this plane, (ii) a straight line representing the TL length is drawn up linking these points directly, so φ_γ is obtained ($\varphi_\gamma = 63.435°$ in the example). The phases verify Eq. (9), so the TL is physically realizable assuming the line parameters ($r = 0.027$ and $g = 1.260$ in the example). With this parameterization, the analysis in both the ρ- and Z_n-planes is completed by transforming the curves from the $\rho_{\log}$-plane (the concrete values of the example are shown in Fig. 5). It is important to remark how the analysis from the $\rho_{\log}$-plane makes the impedance matching easier by means of a complete graphical process. Notice also that the solution achieved is not unique because of the arbitrary selection of φ_{Z_0} and the direct line linking $\rho_{\log L}$ and $\rho_{\log M}$, which provides the shortest TL but not the only one possible. In any case, the analysis in the $\rho_{\log}$-plane also leads to checking the physical realizability in Eq. (9).

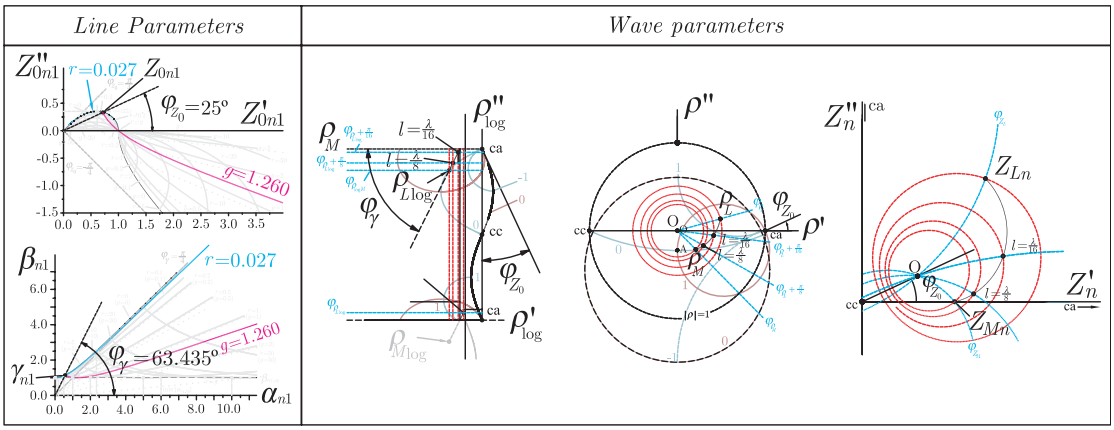

Figure 5. Graphical analysis of the matching procedure from the impedance $Z_L = 2 + 2j$ to the real impedance $Z_M = 1.5$ by using a TL with $\varphi_{Z_0} = 25°$ and $\varphi_\gamma = 63.435°$.

5. CONCLUSION

A new version of the Smith Chart has been introduced in this paper. The $\rho_{\log}$-plane containing the log-GSC has demonstrated its usefulness when trying to analyze the wave parameters along the TL. In this sense, some examples of use have been presented taking advantage of the graphical and geometrical analysis along the TL which the $\rho_{\log}$-plane gives special emphasis to. Splitting the analysis of lossy TLs in propagative and evanescent in the $\rho_{\log}$-plane may be specially important in power balance analysis as well as in the construction of graphical transformations between planes. In addition, by means of the analysis in the $\rho_{\log}$-plane, some practical uses of TLs have been shown taking advantage of the losses when studying them rigorously, alternative to the classical matching techniques based on lossless TLs.

ACKNOWLEDGMENT

This work has been supported by the Spanish "Economía y Competitividad" Ministry under projects TEC2014-54005-P and TEC2016-80815-P.

REFERENCES

1. Gago-Ribas, E., *Complex Transmission Line Analysis Handbook*, Vol. GW-I, "Electromagnetics & Signal Theory Notebooks" series. GR-Editores, León, Spain, 2001.
2. Gago-Ribas, E., P. Vidal-García, and J. Heredia-Juesas, "Complex analysis and parameterization of the lossy transmission line theory and its application to solve related physical problems," *International Conference on Electromagnetics in Advanced Applications, ICEAA 2015 Proceedings*, 141–144, Torino, Italia, September 7–11, 2015.
3. Smith, P. H., "Transmission-line calculator," *Electronics*, Vol. 12, 29, 1939.
4. Smith, P. H., "An improved transmission-line calculator," *Electronics*, Vol. 17, 130, 1944.
5. Gago-Ribas, E., C. Dehesa Martínez, and M. J. González Morales, "Complex analysis of the lossy-transmission line theory: A generalized Smith Chart," *Turkish Journal of Electrical Engineering & Computer Sciences (Elektrik)*, Special issue on Electrical and Computer Engineering Education in the 21st Century; Issues, Perspectives and Challenges, Turkey, Vol. 14, No. 1, 173–194, 2006.
6. Wu, Y., Y. Zhang, and Y. Liu, "Analysis of the omnipotent Smith Chart with imaginary characteristic impedances," *ICMMT 2008 Proceedings*, Nanjing, China, April 2014.
7. Wu, Y., H. Huang, and Y. Liu, "An extended omnipotent Smith Chart with active parameters," *Microwave and Optical Technology Letters*, Vol. 50, No. 4, 896–899, 2008.